Applied Physics A (2022) 128:6
https://doi.org/10.1007/s00339-021-05143-y

Applied Physics A
Materials Science & Processing

Compressible piezoresistive pressure sensor based on Ag nanowires wrapped conductive carbonized melamine foam

Bin Cai[1] · Liying Wang[1] · Fei Yu[1,2] · jianming Jia[1] · Jialun Li[1] · Xuesong Li[1] · Xijia Yang[1] · Yi Jiang[2] · Wei Lü[1,3]

Received: 21 September 2021 / Accepted: 25 November 2021 / Published online: 5 December 2021

Abstract

Wearable sensing technology is receiving great attention due to potential applications in smart electronic devices, which requires the sensors own high sensitivity and flexibility at the same time. In present work, we fabricated piezoresistive sensors with the carbonized melamine foam (CMF) and silver nanowires (AgNWs). The CMF and AgNWs interlace and contact each other to form 3D network structures, thus increasing the conductive path. The CMF provided porous skeleton with elasticity. Due to the synergic effect of CMF and AgNWs, the prepared AgNWs@CMF piezoresistive sensor achieved a high sensitivity (4.97 kpa^{-1} at 30–50 kpa) and excellent stability during cycles within 4000 s (1000 times). Based on the sensor performance tests, it is proved that the AgNWs@CMF pressure sensor can be used to monitor different positions of the human body. This work provided a new opportunity to manufacture CMF based piezoresistive sensors with high-performance in future development of electronic skin.

Keywords Sensor · Carbon electrode · Flexible electronics · Silver

1 Introduction

Due to the advancement of Artificial Intelligence technology and smart electronics, wearable sensing technology has been developed rapidly and widely used in daily life [1–5]. As one of the important components of wearable sensing technology, the flexible pressure sensor has been applied to monitor human movement and health [6]. According to the pressure sensing mechanism, the flexible pressure sensor can be divided into piezoresistive sensor [7–11], capacitive sensor [12–16], piezoelectric sensor [17–20] and triboelectric pressure sensors [21–23]. Among them, the piezoresistive pressure sensors are widely concerned because of their simple structure, convenient preparation, low cost and stable performance. [24, 25].

Sponge is an easy-to-obtain, inexpensive porous elastic material. A conductive porous elastic nanocomposite based on sponge has become potential candidates for piezoresistive sensors. However, the insulating elastic sponge matrix will not work properly when the conductive filler falls off. Therefore, it is particularly necessary to choose a conductive porous elastic matrix. The carbonized melamine foam (CMF) could not only retain the original porous structure of the sponge, but also has good electrical conductivity. Moreover, errors caused by shedding of conductive packing on insulating substrates can be reduced because of the conductivity of substrate. The light weight and hydrophobic properties of carbon-based materials are more in line with the requirements of wearable sensors.

Low initial current and large current output under certain pressure are the key elements to obtain high sensitivity [26]. The conductivity of CMF itself is relatively low. Thereby, it is difficult to obtain a large current output under a certain pressure while obtaining a small initial current, so that high sensitivity cannot be obtained. It is

✉ Liying Wang
wangliying@ccut.edu.cn

✉ Yi Jiang
jiangyi@ccit.edu.cn

[1] Key Laboratory of Advanced Structural Materials (Changchun University of Technology), Ministry of Education and School of Materials Science and Engineering, Changchun University of Technology, Changchun 130012, China

[2] School of Science, Changchun Institute of Technology, Changchun 130012, China

[3] State Key Laboratory of Luminescence and Applications, Fine Mechanics and Physics, Chinese Academy of Sciences, Changchun Institute of Optics, Changchun 130012, China

necessary to add a conductive filler with good conductivity. Due to the conductive mechanism of the electron tunneling process, silver nanowires (AgNWs) have good sensitivity. Compared with carbon nanomaterials, the synthesis of AgNWs is more environmentally friendly and does not require strong acid reagents. At the same time, it is also the conductive filler with the highest neutral price of metal particles in flexible devices.

Here, we show a simple and economical method to manufacture AgNWs@CMF via dip-coating the CMF into a solution including AgNWs. Due to the CMF with relatively low conductivity and AgNWs with suitable loading amount, the conductivity could be adjusted, and an incomplete conductive network ensures a small initial current. When the porous skeleton is subjected to certain pressure, AgNWs wrapped on CMF are connected to each other, forming a closer three-dimensional conductive network. It is coordinated with the contact effect of adjacent skeleton to ensure variable output of large current. The AgNWs@CMF flexible pressure sensor could be used to monitor different movements of the human body as shown later. It has broad application prospects in wearable electronic sensing in the near future.

2 Experimental section

2.1 Preparation of carbonized sponge

First, the commercially available MF foam was cut into numerous pieces, and washed with acetone, ethanol and deionized water. Then, the MFs were dried in an oven at 80 °C for 12 h. To obtain the CMF sponge, the MFs were placed in a tube furnace under nitrogen, and heated to 500 °C temperature for 2 h.

2.2 Preparation of AgNWs@CMF sponge

The synthesis process of AgNWs solution was according to previous reports [27–29]. Soak the CMF in a solution containing AgNWs (5 mg/ml) for 30 min, squeeze out the excess liquid, and then dry it in an oven at 60 °C for 90 min. Repeat this process 5 times to obtain AgNWs@CMF.

3 Results and discussion

The scheme in Fig. 1 illustrates the manufacturing process of AgNWs@CMF. MF is a kind of low-cost and readily available material with good compressibility. Specifically, CMF treated at 500 °C is still able to maintain a good elasticity, and is suitable as a base material of flexible pressure sensors. Due to the conductivity of the CMF flexible matrix, the influence of the conductive filler falling off in the conductive composite material could be avoided. Moreover, CMF inherits the porous structure of MF, the pressure sensor can withstand a wide range of pressure. Given that sensor based on AgNWs has high sensitivity, but susceptible to mechanical deformation stress, the working range and the cycle stability were limited. The composite of CMF and AgNWs could enhance the conductivity of CMF without sacrificing the elasticity of CMF. At the same time, it can also increase the stability of the sensor and reduce the irreversible deformation between AgNWs. [28].

Figure 2a is the digital photograph of the prepared AgNWs with a concentration of 5 mg/ml. Figure 2b is the CMF picture. The CMF sponge can be supported by green leaf without bending, indicating the extremely light weight of CMF. As shown in Fig. 2c, it can be clearly seen that the length of the AgNWs is about 10–20 μm. Figure S1(a) shows the XRD spectrum of AgNWs. Five characteristic diffraction peaks are observed at 2θ = 38.05°, 44.73°, 63.87°, 78.37°

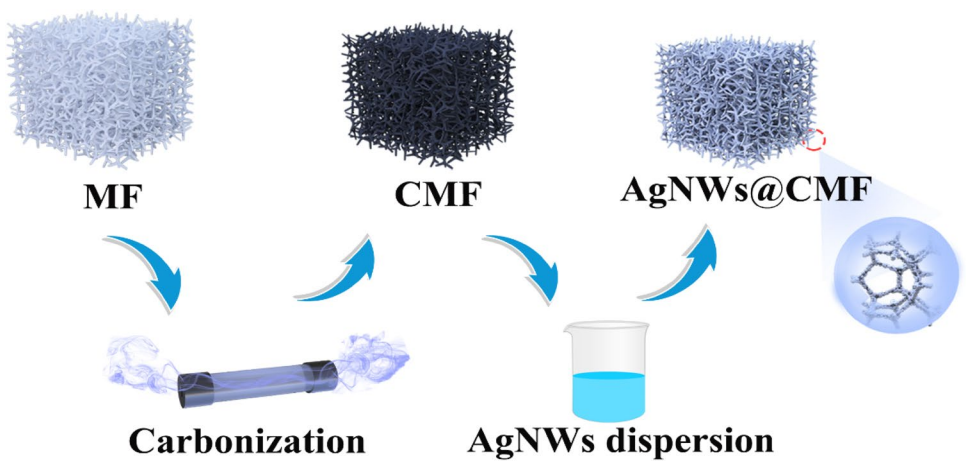

Fig. 1 Illustration for Preparing AgNWs@CMF

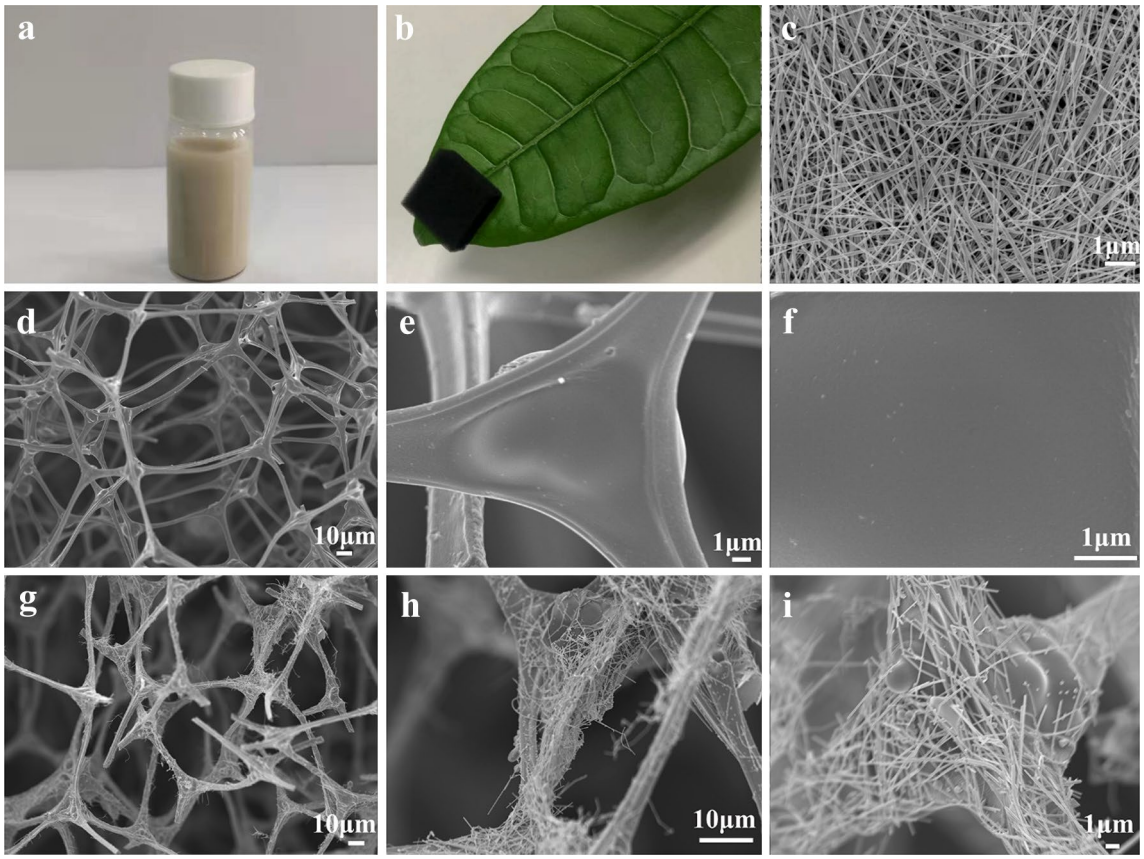

Fig. 2 **a** 5 mg/ml AgNWs solution; **b** CMF supported by green leaf without bending; **c** SEM image of AgNWs; **d–f** SEM images of CMF **g–i** SEM images of AgNWs@CMF

and 81.38°, corresponding to (111), (200), (220), (311) and (222) planes of pure face-centered cubic silver crystals.[8] In Figure S1(b), the absorption peaks at 350 and 400 nm in the UV–vis spectrum are characteristic peaks of AgNWs. Figure 2d–f shows SEM images of the CMF, showing a continuous porous 3D structure, and the surface was smooth. Figure 2g–f is the SEM images of the composite material of AgNWs and CMF. As shown in Figure S4, it can be seen from the absorption spectrum that the CMF absorption intensity of the soaking over silver nanowire is significantly improved. After grinding the AgNWs @ CMF sponge into powder, XRD test is performed. The broad peak around 20° is attributed to carbon, and the peaks at 38.1°, 44.3°, 64.4°, 77.5°, 81.5° can be well indexed to Ag (PDF#04–0783). In addition, we test the stress–strain curve of CMF and AgNWs@CMF, as shown in Figure S5. It can be seen from the figure that AgNWs@CMF can still maintain the same compression performance as CMF.

According to the related research of the pressure sensor, the sensitivity of pressure sensor can be defined as $S = \partial(\Delta I/I_0)/\partial P$, where ΔI is the relative change of current, I_0 is the current of the elastomer without load, and ∂P is the pressure variety. To study the pressure-current response of the AgNWs@CMF sensor, the current variation as a function of applied pressure was recorded in Fig. 3a. The response current of the AgNWs@CMF sensor increases as the applied pressure increases. Obviously, the sensitivity of the sensor can be divided into two parts: I area (0–30 kpa), II area (30–50 kpa). The sensitivity of sensor was 0.79 kpa^{-1} and 4.97 kpa^{-1}, respectively. The main reason was the structural variation inside the AgNWs@CMF sensor. Within the pressure range of 0 to 30 kpa, the resistance of AgNWs@CMF was mainly determined by the CMF matrix, and the contact mode of the conductive porous skeleton was mainly point contact. This can be explained by the change in the number of contact points of the porous structure foam. When pressure was applied to the foam, the porous material skeleton rearranges and the number of contact points between the conductive layers increases. Within the pressure range of 30 to 50 kpa, the resistance of AgNWs@CMF will decrease rapidly. The point contact was no longer the main contact mode between carbonized sponges, and the regional contact become the main contact mode. Due to the tunnel distance decreases between the silver nanowires layers, the tunnel resistance was reduced. To verify the responsiveness of the AgNWs@CMF sensor, pressures of 0, 5, 10, 20, 30, 40, and

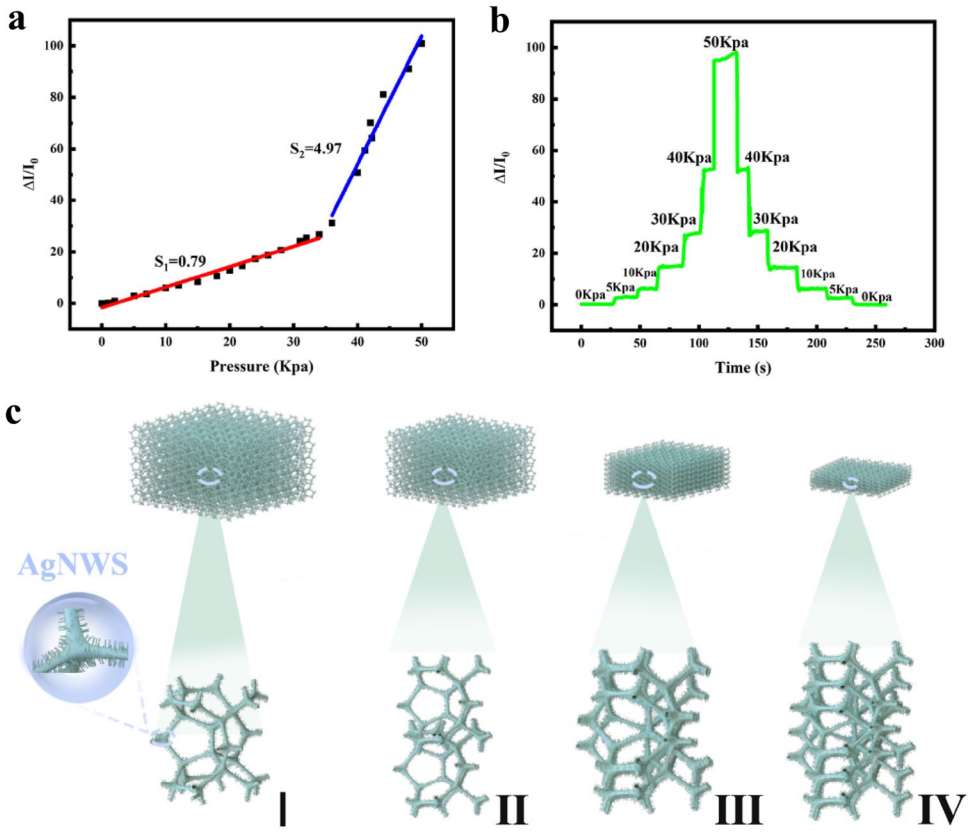

Fig. 3 **a** The $\Delta I/I_0$ of the AgNWs@CMF sensor changes with the increase of pressure. **b** $\Delta I/I_0$ of AgNWs@CMF sensors with different pressures. **c** the schematic diagram of the porous structure with the increasing pressure

50 kpa were applied to the AgNWs@CMF sensor as shown in Fig. 3b. Obviously, the value of $\Delta I/I_0$ increases with the increase in pressure, which is consistent with the results in Fig. 3a. Under the same pressure, the value of $\Delta I/I_0$ is the same, which shows the sensor performance was stable. As mentioned earlier, under the pressure of 30–50 kpa, the value of $\Delta I/I_0$ changes more obviously. Different pressures will change the internal arrangement of the porous framework. It also shows that the internal contact mode of the conductive porous framework is different under different pressures. As shown in Fig. 3c, CMF is a porous material with good electrical conductivity and superior mechanical properties. After being subjected to pressure, the porous framework will be compressed and cause the internal structure change. Initially, the main contact mode is "point contact." It is mainly affected by the performance of the carbonized framework itself, resulting in the number of conductive paths increases sharply, and the resistance decreases. After that, with the increase in compressive strain, "point contact" gradually into "regional contact." When " regional contact" becomes the main contact mode, the porous skeletons of the sponge are in contact to each other. The combined effect of AgNWs on the enhanced conductivity of the carbonized framework and the " regional contact" mode, the resistance decreases rapidly, making the piezoresistive sensor more sensitive. Under pressure, the CMF and the AgNWs will interlace and contact each other to form a 3D network structure, thus increasing the conductive path. Because the conductivity of silver is very high, a large current change output under pressure could be achieved with a small initial current. Therefore, higher sensitivity can be obtained, and the performance of the sensor is guaranteed.

To verify the change in pressure in the schematic diagram of Fig. 3c, stress simulation was performed as shown in Fig. 4 based on finite element analysis. A porous sponge model was built and different pressures were applied (0, 2.38, 3.39, 6.45, 13.6, 19.7, 28.9, 49.3 kpa). Before the pressure is 28.9 kpa, it can be observed that the sponge skeletons have less contact with each other, which is consistent with the initial pressure range of the sensitivity of the second stage of the experiment. At this time, the contact is mainly point contact. Therefore, the main source of the influence of resistance changes is the CMF framework. As the applied pressure increases, the sponge skeleton is compressed severely. The contact between the sponge skeletons changes from point contact to surface contact. From this, analysis shows that the sponge skeleton under high pressure will be in contact with each other, and the surface will be in contact with each other. The resistance decreases rapidly and the sensitivity increases.

Figure 5a shows schematic diagram of a flexible pressure sensor, which consists of two copper foils and AgNWs@

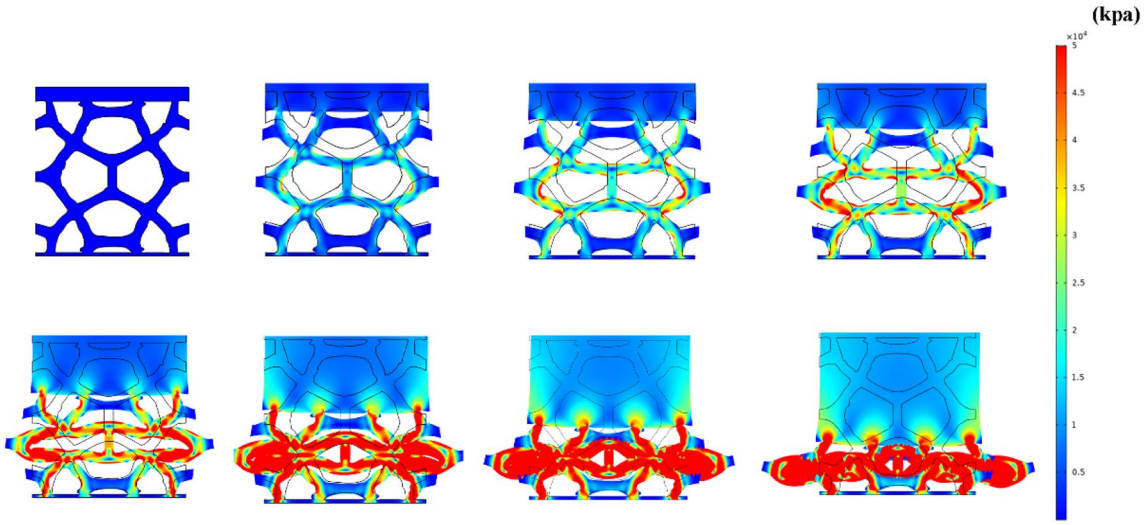

Fig. 4 Finite element analysis of the mechanical properties of the sponge structure under different pressures (0 kpa, 2.38 kpa, 3.39 kpa, 6.45 kpa, 13.6 kpa, 19.2 kpa, 28.9 kpa,49.3kpa)

CMF. As shown in Fig. 5b, the performance of sensors shows different behavior with different concentration of AgNWs. Compared with pure CMF device, the devices with the concentrations of 2 mg/ml and 5 mg/ml show great improvement in performance. However, further increase in concentration induces a performance decay, which is due to the increased conductivity by too much AgNWs in CMF. High concentration of AgNWs will make the sponge a conductor and thus lose its piezoresistive performance. Within the pressure range of 0 to 30 kpa, the performance of AgNWs@CMF pressure sensor is slightly better than that of CMF sensor. Because the AgNWs on CMF can improve the conductivity of the CMF framework. When the pressure is higher than 30 kpa, the main contact mode of the pressure sensor at this time is regional contact. The deformability of porous materials under high pressure is weakened. As the pressure increases, the rate of the mutual contact area increases will decrease. The deformability of the porous structure tends to be saturated, and the number of conductive paths tends to be stable. Thereby, even if the pressure increases, the conductive path remains unchanged, which cause the little current change for CMF sensor. The thickness effect of AgNWs@CMF sensor on performance was explored and shown in Fig. 5c. When the thickness of AgNWs@CMF layer is 3 mm, the thicker matrix layer leads to uneven dispersion of AgNWs. Therefore, the current change caused by the shortening of the distance between the AgNWs layers is lower than that of 2 mm thick AgNWs@CMF. When the thickness of the AgNWs@CMF layer is 1.5 mm, the thinner layer will have excessive loading of AgNWs. As a result, the electrical signal enhancement effect of the AgNWs was weakened. Therefore, the AgNWs@CMF layer thickness of 2 mm is the most suitable value. As shown in Fig. 5d, the current–voltage (I–V) curve of the AgNWs@CMF pressure sensor under different pressures shows good linear ohmic characteristics. Which shows the AgNWs@CMF sensor has stable response ability. As shown in Fig. 5e, the response time of the pressure sensor when loading is ~ 0.3 s, and the recovery time is ~ 0.2 s. Figure 5f shows the brightness change in red LEDs without and with pressure loading. The lighting image on the right hand indicted the conduction status of the sensor under enough sensor.

Figure 5g is the cycling test of electrical signal for 1000 times within 4000 s under a pressure of 20 kpa. The sensor showed remarkable circulation and repeatability with little change after 1000 times. In Fig. 5h and i, the sharp resistance amplitude of the loading and unloading cycles in the first and last 20 s is almost the same, which indicates the sensor performance is stable.

As mentioned above, the flexible AgNWs@CMF sensor has good sensitivity for wearable electronic devices. To confirm this, we have tested it on daily life behaviors. The AgNWs@CMF sensor is fixed at different positions in the human body to tests sensing ability. The response of sensor to human motion is recorded and shown in Fig. 6. The movements of throat, cheek, blowing, elbow, and finger are monitored by the sensor and corresponding results are shown in Fig. 6a–e. Each movement can create a steady change in current, which explains the sensor's ability to monitor tiny movements. Blowing air onto the AgNWs@CMF pressure sensor could observe the obvious change in resistance, which indicates that AgNWs@CMF sensor is efficient in monitoring human breathing. This proves that AgNWs@CMF can be used to monitor tiny movements in the human body.

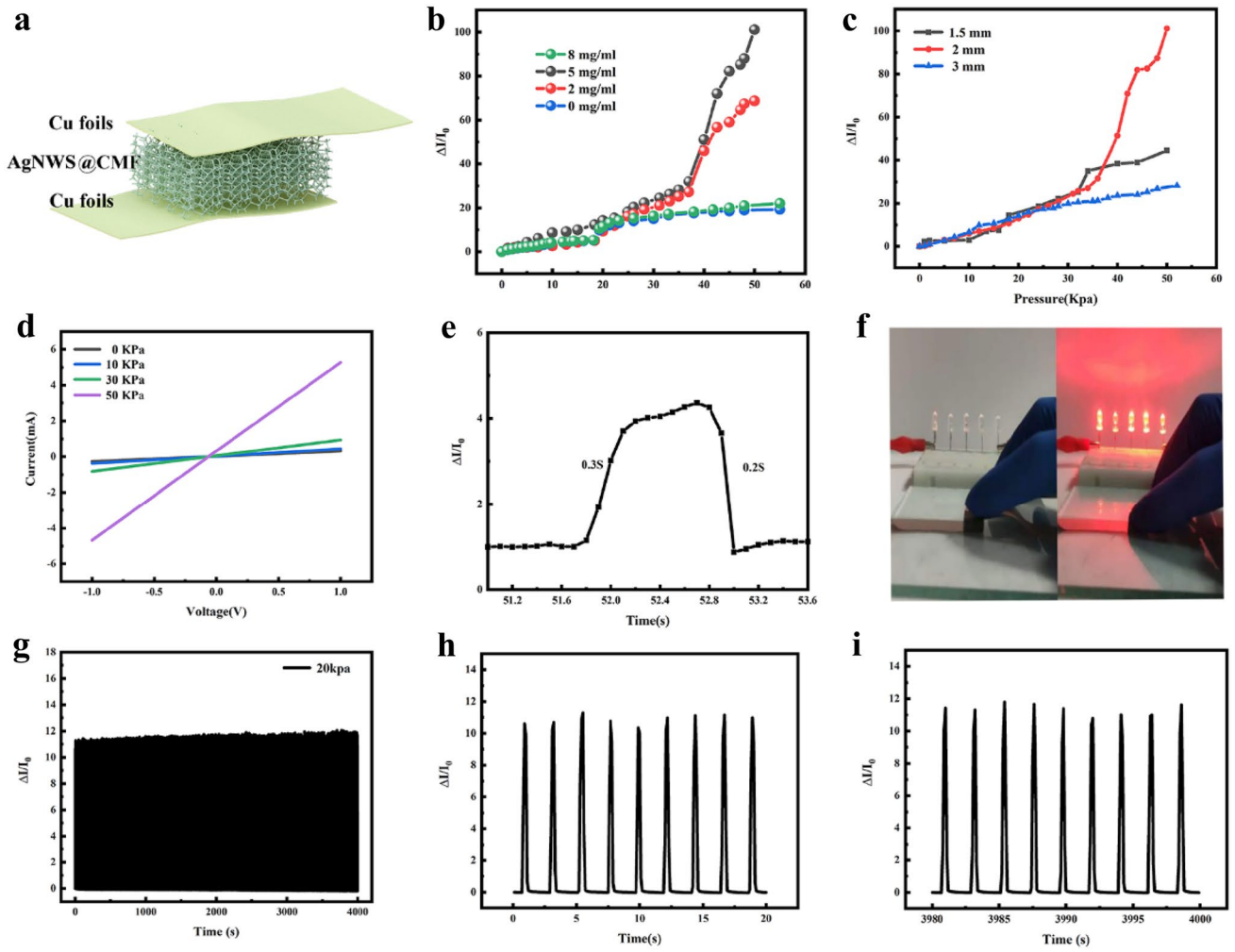

Fig. 5 **a** Schematic diagram of AgNWs@CMF sensor. **b** Influence of different concentrations of AgNWs on sensor performance **c** The change of $\Delta I/I_0$ of pressure sensors with different thicknesses of AgNWs@CMF under different pressures. **d** Current–voltage curve of AgNWs@CMF sensor under different pressures. **e** The response time is about 0.3 s. **f** The brightness change of the small bulb before and after the AgNWs@CMF sensor is pressed. **g** cycling test of AgNWs@CMF sensor under 20 Kpa, **h** the change of ΔI/I0 in the first 20 s, **i** the change of ΔI/I0 in the last 20 s

Figure 6f shows the AgNWs@CMF sensor is placed on the mouse to monitor pressure variation. The current changes with the movement of the finger obviously. The response of sensor to pressure is also tested by attaching it to paper cups with different water loading amount (empty cup and cup filled with water). As shown in Fig. 6g, we test the changes of $\Delta I/I_0$ of the sensor under the above two different conditions. Both the$\Delta I/I_0$ values change obviously when the tester picks up a paper cup, and that of cup filled with water change larger, indicating that the sensor could distinguish the weight difference. In addition, the variation of current with time under different finger motion is tested and shown in Figure S6, which indicates the isotropy of present material.

4 Conclusion

In summary, AgNWs@CMF composite has been synthesized through a simple and low-cost manufacturing process, and is proposed as a key component material for compressible piezoresistive pressure sensor. The sensor exhibited a maximum sensitivity of 4.97 kpa^{-1} at 30–50 kpa, and showed excellent stability over a period of 4000 s (1000 times). This is due to the CMF's three-dimensional network architecture and the greater current variation output of the AgNWs under pressure. The theoretical and experimental analysis both indicate that the contact mode

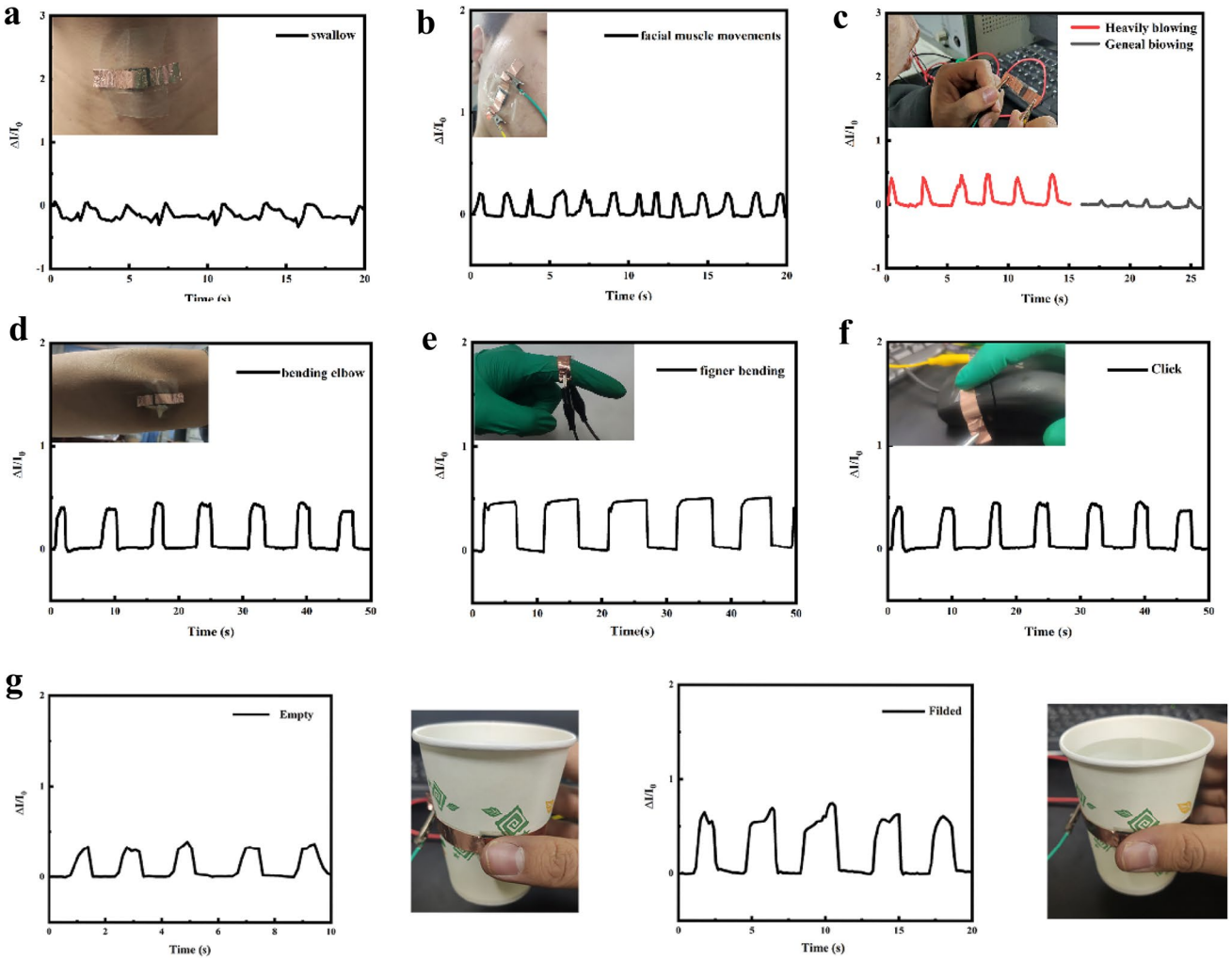

Fig. 6 The resistance changes of AgNWs@CMF pressure sensor in different application scenarios: **a** monitoring the subtle movement of the laryngeal junction, **b** monitoring the subtle movement of the facial muscles, **c** the pressure of the airflow in the oral cavity, **d** monitoring the arm bend, **e** monitor finger bending, **f** monitor finger click and mouse action, **g** monitor the pressure generated by grabbing different weights

between the sponge skeletons changes from point contact to surface contact, which induce two signal variation stages. The prepared sensor is very suitable for monitoring different positions of the human body, such as the face, laryngeal knot, arms, and fingers. This study lays a foundation for the design of pressure sensors, and the improvement of performance of wearable electronic.

Supplementary Information The online version contains supplementary material available at https://doi.org/10.1007/s00339-021-05143-y.

Acknowledgements This research was supported by grants from the National Natural Science Foundation of China (No. 62004015 and 62004014), Science and Technology Research Project of Jilin Provincial Department of Education (JJKH20210735KJ)

Declarations

Conflict of interest The authors declare that they have no known competing financial interest or personal relationships that could have appeared to influence the work reported in this paper.

References

1. J.R. Jung, S.I. Ahn, Van der Waals pressure sensors using reduced graphene oxide composites. Chem. Phys. Lett. **697**, 12–16 (2018). https://doi.org/10.1016/j.cplett.2018.02.058
2. Y. Zhang, M. Li, X. Han, Z. Fan, H. Zhang, Q. Li, High-strength and highly electrically conductive hydrogels for wearable strain sensor. Chem. Phys. Lett. (2021). https://doi.org/10.1016/j.cplett.2021.138437

3. X. Hou, Q. Zhang, L. Wang, G. Gao, W. Lu, Low-temperature-resistant flexible solid supercapacitors based on organohydrogel electrolytes and microvoid-incorporated reduced graphene oxide electrodes. ACS Appl. Mater. Interfaces **13**, 12432–12441 (2021). https://doi.org/10.1021/acsami.0c18741
4. L. Duan, L. Zhao, H. Cong, X. Zhang, W. Lu, C. Xue, Plasma treatment for nitrogen-doped 3D graphene framework by a conductive matrix with sulfur for high-performance Li-S batteries. Small **15**, e1804347 (2019). https://doi.org/10.1002/smll.201804347
5. X.Y. Zhang, S.H. Sun, X.J. Sun, Y.R. Zhao, L. Chen, Y. Yang, W. Lu, D.B. Li, Plasma-induced, nitrogen-doped graphene-based aerogels for high-performance supercapacitors. Light Sci. Appl. **5**, e16130 (2016). https://doi.org/10.1038/lsa.2016.130
6. Y. Ding, T. Xu, O. Onyilagha, H. Fong, Z. Zhu, Recent advances in flexible and wearable pressure sensors based on piezoresistive 3D monolithic conductive sponges. ACS Appl. Mater. Interfaces **11**, 6685–6704 (2019). https://doi.org/10.1021/acsami.8b20929
7. S. Zhang, H. Liu, S. Yang, X. Shi, D. Zhang, C. Shan, L. Mi, C. Liu, C. Shen, Z. Guo, Ultrasensitive and highly compressible piezoresistive sensor based on polyurethane sponge coated with a cracked cellulose nanofibril/silver nanowire layer. ACS Appl Mater. Interfaces **11**, 10922–10932 (2019). https://doi.org/10.1021/acsami.9b00900
8. X.P. Li, Y. Li, X. Li, D. Song, P. Min, C. Hu, H.B. Zhang, N. Koratkar, Z.Z. Yu, Highly sensitive, reliable and flexible piezoresistive pressure sensors featuring polyurethane sponge coated with MXene sheets. J. Colloid Interface Sci. **542**, 54–62 (2019). https://doi.org/10.1016/j.jcis.2019.01.123
9. T. Xia, R. Yu, J. Yuan, C. Yi, L. Ma, F. Liu, G.J. Cheng, Ultrahigh sensitivity flexible pressure sensors based on 3D-printed hollow microstructures for electronic skins. Adv. Mater. Technol. (2021). https://doi.org/10.1002/admt.202000984
10. J. Meng, P. Pan, Z. Yang, J. Wei, Q. Wang, M. Gong, G. Zhang, Degradable and highly sensitive CB-based pressure sensor with applications for speech recognition and human motion monitoring. J. Mater. Sci. **55**, 10084–10094 (2020). https://doi.org/10.1007/s10853-020-04707-2
11. M. Liu, X. Pu, C. Jiang, T. Liu, X. Huang, L. Chen, C. Du, J. Sun, W. Hu, Z.L. Wang, Large-area all-textile pressure sensors for monitoring human motion and physiological signals. Adv. Mater. (2017). https://doi.org/10.1002/adma.201703700
12. J. Yang, S. Luo, X. Zhou, J. Li, J. Fu, W. Yang, D. Wei, Flexible, tunable, and ultrasensitive capacitive pressure sensor with microconformal graphene electrodes. ACS Appl Mater Interfaces **11**, 14997–15006 (2019). https://doi.org/10.1021/acsami.9b02049
13. S. Kang, J. Lee, S. Lee, S. Kim, J.-K. Kim, H. Algadi, S. Al-Sayari, D.-E. Kim, D. Kim, T. Lee, Highly sensitive pressure sensor based on bioinspired porous structure for real-time tactile sensing. Adv. Electron. Mater. (2016). https://doi.org/10.1002/aelm.201600356
14. J. Qiu, X. Guo, R. Chu, S. Wang, W. Zeng, L. Qu, Y. Zhao, F. Yan, G. Xing, Rapid-response, low detection limit, and high-sensitivity capacitive flexible tactile sensor based on three-dimensional porous dielectric layer for wearable electronic skin. ACS Appl. Mater. Interfaces **11**, 40716–40725 (2019). https://doi.org/10.1021/acsami.9b16511
15. Q. Zhang, W. Jia, C. Ji, Z. Pei, Z. Jing, Y. Cheng, W. Zhang, K. Zhuo, J. Ji, Z. Yuan, S. Sang, Flexible wide-srange capacitive pressure sensor using micropore PE tape as template. Smart Mater. Struct. (2019). https://doi.org/10.1088/1361-665X/ab4ac6
16. Z. Yuan, G. Shen, C. Pan, Z.L. Wang, Flexible sliding sensor for simultaneous monitoring deformation and displacement on a robotic hand/arm. Nano Energy (2020). https://doi.org/10.1016/j.nanoen.2020.104764
17. J. Sun, X. Zhang, Y. Lang, J. Bian, R. Gao, P. Li, Y. Wang, C. Li, Piezo-phototronic effect improved performance of n-ZnO nanoarrays/p-Cu2O film based pressure sensor synthesized on flexible Cu foil. Nano Energy **32**, 96–104 (2017). https://doi.org/10.1016/j.nanoen.2016.12.028
18. W. Wu, X. Wen, Z.L. Wang, Taxel-addressable matrix of vertical-nanowire piezotronic transistors for active and adaptive tactile imaging. Science **340**, 952–957 (2013). https://doi.org/10.1126/science.1234855
19. W. Choi, J. Kim, E. Lee, G. Mehta, V. Prasad, Asymmetric 2D MoS2 for scalable and high-performance piezoelectric sensors. ACS Appl. Mater. Interfaces **13**, 13596–13603 (2021). https://doi.org/10.1021/acsami.1c00650
20. G.-H. Feng, C.-Y. Chiang, Magnetic-repulsion-coupled piezoelectric-film-based stretchable and flexible acoustic emission sensor. Smart Mater. Struct. (2020). https://doi.org/10.1088/1361-665X/ab67ca
21. F.R. Fan, L. Lin, G. Zhu, W. Wu, R. Zhang, Z.L. Wang, Transparent triboelectric nanogenerators and self-powered pressure sensors based on micropatterned plastic films. Nano Lett **12**, 3109–3114 (2012). https://doi.org/10.1021/nl300988z
22. X.S. Zhang, M.D. Han, R.X. Wang, F.Y. Zhu, Z.H. Li, W. Wang, H.X. Zhang, Frequency-multiplication high-output triboelectric nanogenerator for sustainably powering biomedical microsystems. Nano Lett **13**, 1168–1172 (2013). https://doi.org/10.1021/nl3045684
23. N. Tang, C. Zhou, D. Qu, Y. Fang, Y. Zheng, W. Hu, K. Jin, W. Wu, X. Duan, H. Haick, A highly aligned nanowire-based strain sensor for ultrasensitive monitoring of subtle human motion. Small **16**, e2001363 (2020). https://doi.org/10.1002/smll.202001363
24. G. Ge, Y. Cai, Q. Dong, Y. Zhang, J. Shao, W. Huang, X. Dong, A flexible pressure sensor based on rGO/polyaniline wrapped sponge with tunable sensitivity for human motion detection. Nanoscale **10**, 10033–10040 (2018). https://doi.org/10.1039/c8nr02813c
25. L. Gao, C. Zhu, L. Li, C. Zhang, J. Liu, H.D. Yu, W. Huang, All paper-based flexible and wearable piezoresistive pressure sensor. ACS Appl. Mater. Interfaces **11**, 25034–25042 (2019). https://doi.org/10.1021/acsami.9b07465
26. Z. Wang, S. Guo, H. Li, B. Wang, Y. Sun, Z. Xu, X. Chen, K. Wu, X. Zhang, F. Xing, L. Li, W. Hu, The semiconductor/conductor interface piezoresistive effect in an organic transistor for highly sensitive pressure sensors. Adv. Mater. **31**, e1805630 (2019). https://doi.org/10.1002/adma.201805630
27. H. Jeong, Y. Noh, S.H. Ko, D. Lee, Flexible resistive pressure sensor with silver nanowire networks embedded in polymer using natural formation of air gap. Compos. Sci. Technol. **174**, 50–57 (2019). https://doi.org/10.1016/j.compscitech.2019.01.028
28. Y. Wei, S. Chen, Y. Lin, X. Yuan, L. Liu, Silver nanowires coated on cotton for flexible pressure sensors. J. Mater. Chem. C **4**, 935–943 (2016). https://doi.org/10.1039/c5tc03419a
29. L. Bi, Z. Yang, L. Chen, Z. Wu, C. Ye, Compressible AgNWs/Ti3C2Tx MXene aerogel-based highly sensitive piezoresistive pressure sensor as versatile electronic skins. J. Mater. Chem. A **8**, 20030–20036 (2020). https://doi.org/10.1039/d0ta07044k